10

Frequency band of an acousto-optic fiber modulator with focusers: comparison of experimental data with calculated ones

© V.M. Epikhin[1], P.V. Karnaushkin[2], M.M. Mazur[1], L.I. Mazur[1], L.L. Paltsev[1], V.N. Shorin[1], A.V. Aprelev[1]

[1] All-Russian Research Institute of Physical-Technical and Radiotechnical Measurements, Mendeleevo, Moscow oblast, Russia
[2] Perm State University, Perm, Russia
E-mail: epikvm@mail.ru

Received May 7, 2024
Revised July 5, 2024
Accepted July 28, 2024

A series of acousto-optic modulators with single-mode fiber output-focusing leads has been experimentally investigated. The emission wavelength was 1550 nm, the center frequency of the control signal $\simeq 150$ MHz. The variable parameters were: acoustic wave velocity (different acousto-optic crystals were used), working distance of the focusers, and type of focusing element (gradient and aspherical lenses). In all cases, the measured values of the modulator operating bandwidth within errors coincide with the data calculated within the framework of the previously proposed model.

Keywords: modulator frequency bandwidth, transmission coefficient, optical contrast, acousto-optic crystal, ultrasonic wave velocity, gradient and aspheric lenses.

DOI: 10.61011/TPL.2024.11.59676.19983

Optimization of broadband acousto-optic modulators with single-mode fiber guides (AOMFs) is relevant both to the design of laser cooling systems and stabilization of laser sources [1,2] and to the formation of a short front of a diffracted light pulse in fiber laser ranging applications [3,4]. There is presently an urgent need for a transportable optical frequency standard with a relative instability at the level of $\sim 10^{-16}$–10^{-17}, which was achieved in stationary devices. The solution to this problem involves substituting free-space optical circuits with more physically and informationally secure fiber-optic lines, which are also less susceptible to external influences, with the necessary optical units (in particular, acousto-optic modulators/frequency shifters) integrated into them.

Operating frequency range (frequency band) Δf is an important parameter of an AOMF. For example, an AOMF may be used to obtain a controlled frequency shift of diffracted light within operating band $\Delta f = (f_0 + \Delta f/2) - (f_0 - \Delta f/2)$, where f_0 and Δf are the constant and variable parts of the shift. According to the data reported in [5], the following relation holds true for AOMFs:

$$\Delta f \simeq \min\left(\Delta f_m, \Delta f_{af}, \Delta f_r\right), \qquad (1)$$

where the band frequency characteristics of an actual AOMF are listed in brackets: Δf_m is the matching band of an ultrasonic wave (USW) emitter with the radio-frequency (RF) control signal path; Δf_{af} is the synchronism band or the width of the frequency instrument function of an acousto-optic cell (AOC), which is inversely proportional to the distance of the acousto-optic (AO) interaction; and Δf_r is the reception band within which the power of a diffracted light beam is transmitted to a receiving fiber-optic light guide (FOG) with losses lower than 3 dB [4]. This characteristic is specific to AOMFs, since it is not found in classical (free-space) acousto-optic modulators. In view of (1), term Δf_r governs the formation of Δf in most practically relevant cases.

It was demonstrated theoretically and experimentally in [5] that AOMF reception band Δf_r may be expanded dramatically by switching from collimators to focusers. It is not without interest to perform an additional experimental study of acousto-optic modulators with fiber focusing leads (AOMFFs) with the object of verifying the Δf_r formation model.

The aim of the present study is to compare the measured frequency bands for a series of AOMFs fabricated based on different AO crystals and having different design features with the corresponding data calculated within the proposed model.

The figure shows the optical AOMF circuit (a) and the axisymmetric field angles of a diffracted light beam in the plane orthogonal to axis O_1 (b). Here, F_1 and F_2 are the emitting and receiving focusers; $2w$ is the light beam waist at the AOC center; α is the distance from the lens to the FOG fiber end; α' is the working distance of focusers; NA is the effective numerical aperture of the FOG; V is the USW velocity; λ is the radiation wavelength in air; $M = 2w/D$ is the magnification of the optical system; D is the mode spot size of the FOG; and θ_B is the Bragg angle.

The mechanism of formation of reception frequency band Δf_r consists in limiting the aperture of a diffracted beam when it is introduced into receiving FOG F_2 due to the angular drift of the beam optical axis with a change in frequency f of the control signal. Note that linear and

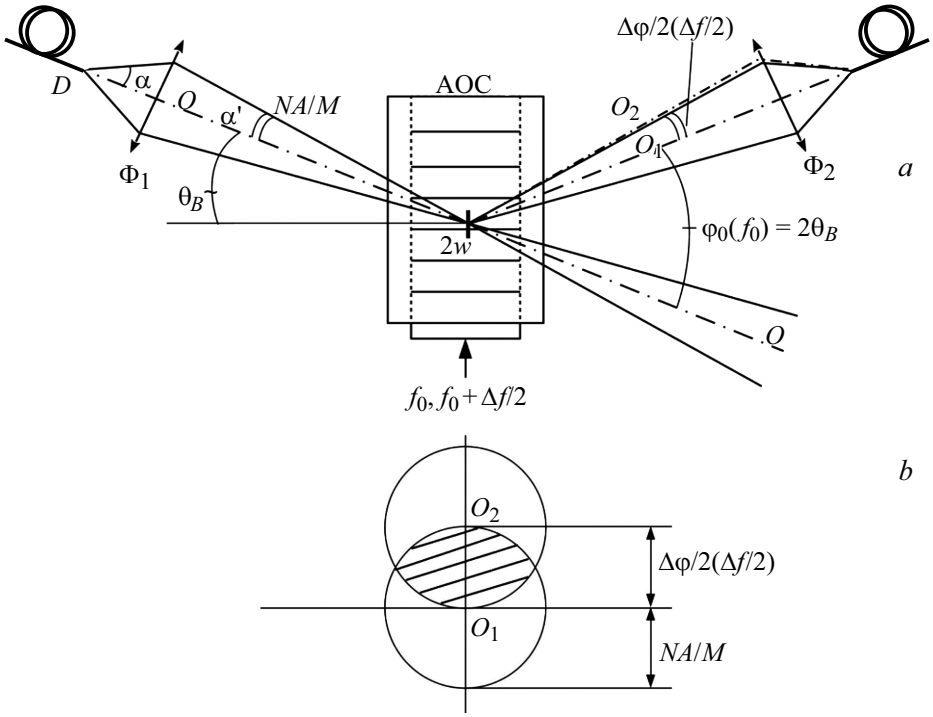

a — Optical circuit of an AOMF with light beam focusing; *b* — arrangement of optical axes O_1 and O_2 and field angles of a diffracted beam at control signal frequencies f_0 and $f_0 + NA \cdot V/(M\lambda)$.

angular apertures are limited in this case for AOMFs with collimators and focusers, respectively [4,5].

Arranged within the AOMFF housing are an AOC, a device for matching the impedances of a piezoelectric transducer (PT) and the RF path (50 Ω), and lens or gradient focusers mounted at the required angle and fitted with fiber-optic cables ending with FC/APC optical connectors. An SMA RF connector for the control signal is also located on the housing.

The fabricated AOMFFs had the following design features.

1. Inequality $\Delta f \simeq \Delta f_r < (\Delta f_{af}, \Delta f_m)$ was satisfied for all the AOMFF samples; i.e., their operating band Δf was specified by reception band Δf_r. All the indicated band frequency characteristics were determined at the level of −3 dB. In the present case, according to [5]:

$$\Delta f_r \approx 1.6\, NA \cdot V/(M\lambda). \qquad (2)$$

The values of λ, NA, and M remained constant for all the AOMFF samples, since they are set by the FOG type used and active transverse AOC aperture $h \simeq 2w = 0.12$ mm, which were fixed by the specific conditions of further application of the AOMFF samples. These values are $\lambda = 1550$ nm, $NA = 0.094$, and $M = 11.5$. In contrast, parameter V was varied. Two types of AO crystals with different values of USW velocity V were used for this purpose: TeO_2 with $V = 4.3 \cdot 10^3$ m/s [6] and $LiBi(MoO_4)_2$ with $V = 3.46 \cdot 10^3$ m/s [7]. This made it possible to verify thoroughly the validity of formula (1).

2. Isotropic diffraction by a longitudinal USW propagating along the Z axis of the crystal was used for all AOMFF types. The piezoelectric transducer dimensions were $h \times l = 0.12 \times 3.5$ mm for the TeO_2 crystal and 0.12×3.0 mm for the $LiBi(MoO_4)_2$ crystal, where l is the PT length along the light beam propagation direction. The diffraction regime was close to the Bragg one: $Q = l\lambda f^2/(nV^2) > 2$ [8]. The ratio of diffraction divergences of light and sound in the diffraction plane is $a \simeq 1$, and the maximum achievable diffraction efficiency is $\simeq 80\%$ [8].

3. The waist of a Gaussian beam located in the middle of the sound column in the near field of the PT is the source of diffracted radiation in the considered model. The actual source is extended, and its boundaries are located at a distance of $\pm l/2$ from the waist along the direction of the light beam propagation. The loss in introduction of radiation from the boundary sections of the source into the fiber are small if the following condition [9] is satisfied:

$$l \ll b = 2z_r = (2w)^2 \pi n/(2\lambda), \qquad (3)$$

where z_r is the Rayleigh length and n is the refraction index of the AO medium. It was estimated that $l/b \simeq 0.05 \ll 1$ for the examined AOMFFs. Note that (3) does not include focuser working distance α'. This implies that the main AOMFF parameters should not depend on α'.

4. Fiber focusers produced by OZ Optics were used [10]. A focuser is an SMF-28 fiber cable with a microlens and an FC/APC optical connector at its ends. The focuser codes are listed in the table (column 3) and contain the following

Main parameters of the studied AOMFFs

AOMFF number	AO crystal	Focuser type	f, MHz	σ, dB	Δf_{af}^{calc}, MHz	Δf_{m}^{exp}, MHz	Δf_{r}^{calc}, MHz	Δf_{r}^{exp}, MHz	K, dB	P, W
1	*2*	*3*	*4*	*5*	*6*	*7*	*8*	*9*	*10*	*11*
1	TeO_2	LPF-01-1550-9/125-S-12-22-1.81GR-55-3A-1-1	152.2	−2.5	88 ± 6	76 ± 1	37 ± 3	38.0 ± 0.5	$\leqslant -59$	2.3
2	TeO_2	LPF-01-1550-9/125-S-11-23-2AS-60-3A-1-1	147.8	−2.4	88 ± 6	100 ± 1	37 ± 3	36.0 ± 0.5	$\leqslant -58$	2.0
3	TeO_2	LPF-01-1550-9/125-S-12-17-1.4AS-60-3A-1-1	149.7	−2.5	88 ± 6	100 ± 1	37 ± 3	35.0 ± 0.5	$\leqslant -59$	2.3
4	$LiBi(MoO_4)_2$	LPF-01-1550-9/125-S-12-10-1.01GR-55-3A-1-1	148.2	−3.6	66 ± 5	100 ± 1	29 ± 2	30.0 ± 0.5	$\leqslant -58$	2.9
5	$LiBi(MoO_4)_2$	LPF-01-1550-9/125-S-11-23-2AS-60-3A-1-1	163.6	−2.3	66 ± 5	68 ± 1	29 ± 2	30.0 ± 0.5	$\leqslant -59$	3.1

information (in sequence): name (collimator, focuser); microlens design code; center of the working wavelength interval (in nm); FOG core and cladding diameters (in μm); FOG type (S — does not support polarization); magnification M of the optical system; working distance α' of the focuser (in mm); focal length F of the focuser (in mm); lens type (GR — gradient, AS — aspherical); backreflection level (in dB); type of processing of the end face of the FOG core — 3A (APC); type and diameter of the FOG jacket (in mm); and FOG length (in m).

Different types of focusing elements (aspherical and gradient lenses) were tested to compare the quality of focusing of the light beam into the waist at the AOC center. The values of transmission coefficient σ and frequency band Δf_r were used to assess the focusing quality.

5. A high-precision hardware and software complex, which was characterized in [4] in experiments with collimators, was used to couple the AOC to the focusers. In the present case, the task was complicated by the need for additional adjustment in the process of selection of working distance α'. Note that the errors in spatial and angular positioning of the hardware and software complex used were $0.1\,\mu$m and $3.6''$.

The parameters were measured in the stationary frequency shifter mode with a change in frequency f of the harmonic control signal [4] (as is the case with AOMFs used in laser cooling systems). Stationarity is understood here as the fulfillment of inequality $\tau \gg 2w/V$ (τ is the time of frequency tuning within the Δf range).

The results of examination of the main AOMFF parameters are listed in the table. As was noted above, the focuser code in the manufacturer's format [10] is given in column 3. The values of center frequency f of the measured band are listed in column 4. Column 5 contains the values of AOMFF transmission coefficient σ obtained at control signal power P (column 11). Coefficient σ was calculated as $\sigma = \lg(I/I_0)$, where I is the maximum achievable (by varying P) radiation power measured in the emitter−AOMFF−receiver arrangement; and I_0 is the value measured in the emitter−FOG−receiver arrangement. An LP 1550-SAD2 laser with an SMF-28 output fiber cable with an FC/APC optical connector was the emitter; a PM20C radiation power meter was the receiver; and an SMF-28 cable section terminated with FC/APC connectors was the FOG. Column 6 presents the AO synchronism bandwidths (at the -3 dB level) calculated using the following formula [11]: $\Delta f_{af}^{calc} = 1.77V^2 n/(lf\lambda)$. Column 7 lists PT matching bandwidths Δf_m^{exp} measured for a standing wave ratio of 5.6 (with the power transmitted into the AOC being at the level of -3 dB of the RF power supplied from the generator) [11]. Reception bandwidth Δf_r^{calc} calculated at the level of -3 dB using formula (2) is presented in column 8. The calculation error was determined by the accuracy of values of parameters NA, V, and M. Reception bandwidth Δf_r^{exp} measured at the level of -3 dB is given in column 9. Column 10 lists the optical contrast values calculated as $K = 10\lg(I_{P=0}/I)$, where $I_{P=0}$ is the radiation power with zero RF signal.

It follows from the table that (1) the values of transmission coefficient σ do not exceed those typical of AOMFs with collimators [4]; (2) the measured and calculated frequency bandwidths match within the corresponding error limits; (3) the values of Δf and σ are virtually independent of focuser working distance α'; and (4) no noticeable influence of the design of the focusing element (gradient or aspherical lens) on parameters Δf, σ, and K was detected.

The following conclusions may be drawn from the obtained results.

1. The technique of coupling the AOC to the FOG [4] is equally efficient for collimators and focusers.

2. The frequency bandwidths measured for all the tested AOMFFs match the calculated ones within the error limits (the data from [5] combined with the results obtained here). Note that the following parameter values were used in [5]: $\lambda = 1064\,\text{nm}$, $NA = 0.11$, and $M = 19.4$. Thus, all parameters included in formula (2) were varied in the aggregate study.

3. Since the main AOMFF parameters do not depend on α' and the focusing element type, one is free to construct compact AOMFFs and use gradient focusers, which are the most stable, resistant to external influences, and inexpensive. For example, the overall dimensions of the housing of AOMFF No. 4 were $44 \times 36 \times 14\,\text{mm}$.

Conflict of interest

The authors declare that they have no conflict of interest.

References

[1] A.V. Semenko, G.S. Belotelov, D.V. Sutyrin, S.N. Slyusarev, V.I. Yudin, A.V. Taichenachev, V.D. Ovsiannikov, V.G. Pal'chikov, Quantum Electron., **51** (6), 484 (2021). DOI: 10.1070/QEL17585.

[2] D.V. Sutyrin, A.Yu. Gribov, R.I. Balaev, A.A. Gorokhina, V.G. Pal'chikov, A.N. Malimon, S.N. Slyusarev, Quantum Electron., **52** (6), 498 (2022). DOI: 10.1070/QEL18058.

[3] T.O. Lukashova, O.E. Nanii, S.P. Nikitin, V.N. Treshchikov, Quantum Electron., **50** (9), 882 (2020). DOI: 10.1070/QEL17225.

[4] V.M. Epikhin, P.V. Karnaushkin, Quantum Electron., **50** (10), 962 (2020). DOI: 10.1070/QEL17378.

[5] V.M. Epikhin, A.V. Ryabinin, Tech. Phys., **66** (7), 864 (2021). DOI: 10.61011/TPL.2024.11.59676.19983
[V.M. Epikhin, A.V. Ryabinin, Tech. Phys., **66**, 864 (2021). DOI: 10.1134/S1063784221060062].

[6] A.A. Blistanov, V.S. Bondarenko, N.V. Perelomova, M.P. Shaskol'skaya, *Akusticheskie kristally* (Nauka, M., 1982), p. 251 (in Russian).

[7] M.M. Mazur, L.I. Mazur, V.N. Shorin, A.A. Pavlyuk, L.L. Pal'tsev, Al'm. Sovrem. Metrol., No. 1 (37), 162 (2024) (in Russian).

[8] L.N. Magdich, I.Ya. Molchanov, *Akustoopticheskie ustroistva i ikh primenenie* (Sov. Radio, M., 1978), p. 26 (in Russian).

[9] J. Eichler, H.J. Eichler, *Lazery. Ispolnenie, upravlenie, primenenie* (Tekhnosfera, M., 2012), p. 241 (in Russian).

[10] *OZ Optics Ltd.* [Electronic source]. www.ozsoptics.com

[11] E. Dieulesaint, D. Royer, *Uprugie volny v tverdykh telakh* (Nauka, M., 1982), p. 338 (in Russian).

Translated by D.Safin